JACS
JOURNAL OF THE AMERICAN CHEMICAL SOCIETY
Article
pubs.acs.org/JACS

Self-Healing, Self-Assembled β-Sheet Peptide–Poly(γ-glutamic acid) Hybrid Hydrogels

David E. Clarke,[†,‡,∥] E. Thomas Pashuck,[†,‡,∥] Sergio Bertazzo,[†,‡] Jonathan V. M. Weaver,[†,§,⊥] and Molly M. Stevens*[,†,‡,§]

[†]Department of Materials, [‡]Institute of Biomedical Engineering, and [§]Department of Bioengineering, Imperial College London, Exhibition Road, London, SW7 2AZ, U.K.

Supporting Information

ABSTRACT: Self-assembled biomaterials are an important class of materials that can be injected and formed *in situ*. However, they often are not able to meet the mechanical properties necessary for many biological applications, losing mechanical properties at low strains. We synthesized hybrid hydrogels consisting of a poly(γ-glutamic acid) polymer network physically cross-linked via grafted self-assembling β-sheet peptides to provide non-covalent cross-linking through β-sheet assembly, reinforced with a polymer backbone to improve strain stability. By altering the β-sheet peptide graft density and concentration, we can tailor the mechanical properties of the hydrogels over an order of magnitude range of 10−200 kPa, which is in the region of many soft tissues. Also, due to the ability of the non-covalent β-sheet cross-links to reassemble, the hydrogels can self-heal after being strained to failure, in most cases recovering all of their original storage moduli. Using a combination of spectroscopic techniques, we were able to probe the secondary structure of the materials and verify the presence of β-sheets within the hybrid hydrogels. Since the polymer backbone requires less than a 15% functionalization of its repeating units with β-sheet peptides to form a hydrogel, it can easily be modified further to incorporate specific biological epitopes. This self-healing polymer−β-sheet peptide hybrid hydrogel with tailorable mechanical properties is a promising platform for future tissue-engineering scaffolds and biomedical applications.

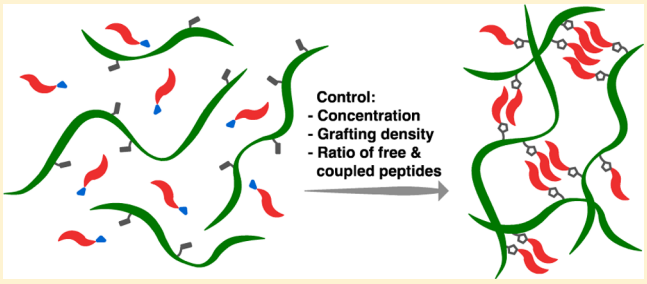

INTRODUCTION

Tissue-engineering strategies commonly utilize a biomimetic scaffold material that provides mechanical support for cells and allows for functionalization with bioactive moieties that elicit a desired cellular response.[1] These scaffolds are typically made from soft materials, such as polymer or peptide hydrogels, which encapsulate cells and allow for cell migration and nutrient diffusion. Covalently cross-linked polymer hydrogels generally have more robust mechanical properties, with weak gels having moduli below a kilopascal to tough hydrogels having moduli of several megapascals. These properties can be tailored through concentration, cross-linking density, or molecular architecture.[2,3] However, these hydrogels are often made of non-natural monomers and either require surgical implantation or typically need to be polymerized or cross-linked *in situ* when injected. Self-assembled hydrogels are most often made from peptides and have some advantages over many covalently cross-linked hydrogels. They can often be injected, and gelation is typically induced by ions present in physiological solutions or added separately. Since their assembly is governed through non-covalent interactions, these can recover over 90% of their mechanical properties after being strained to failure.[4] They also have advantages in biocompatibility, degrading into natural amino acids, and multiple bioactive epitopes can be easily incorporated.[5−8] However, in physiological conditions they suffer from low failure strains, which can be problematic for applications which require resistance to strain, and generally cells can exert significant force on their local environment.[9]

Polymers conjugated with peptides are widely used in tissue-engineering applications.[10,11] In most cases the peptide sequences bind to cells to promote a specific biological response, such as cell adhesion[12] or receptor signaling.[13] However, peptides can also be utilized to modify the mechanical properties of hydrogels through non-covalent interactions. This can create a hybrid hydrogel that has the strain-resistance of a polymer hydrogel but can recover and assemble like a peptide hydrogel. Non-covalent interactions have been successfully used to provide added functionality and responsiveness to polymer networks, especially in shear-thinning and the ability to self-heal.[14−19] Many cells in living tissues experience a wide range of mechanical environments present under physiological conditions, adding complexity when engineering a scaffold for such tissues. One way to approach this engineering problem would be to develop a scaffold that can self-heal, providing a recovery in mechanical properties following an exposure to large strains. In previous

Received: January 25, 2017
Published: May 19, 2017

DOI: 10.1021/jacs.7b00528
J. Am. Chem. Soc. 2017, 139, 7250−7255

work, peptides designed to guide the organization of polymer networks through peptide self-assembly have included coiled-coils[20−22] and β-sheets.[23−25] Specifically the self-assembly of β-sheets motifs have been utilized in block copolymers[26−28] as nanofiber-forming grafts to synthetic polymer networks[29,30] and as cross-links in hydrogels.[31−34] We hypothesized that the use of non-covalent β-sheet peptide cross-links would provide the necessary driving force to reassemble polymer chains following large strains. Furthermore, since the strength of the non-covalent cross-links is dependent on the composition of the peptide sequence, we could tailor the properties of the hydrogel by changing both the number of grafted peptides and the strength of the individual interactions.

Here we present a biodegradable polymer−peptide hydrogel consisting of a poly(γ-glutamic acid) (γ-PGA) polymer network physically cross-linked via conjugated β-sheet peptide sequences (Figure 1A). γ-PGA is a naturally occurring homopolypeptide that is produced by bacteria and archaea and is enzymatically degradable, highly biocompatible, and water soluble.[35,36] In previous work we have shown that derivatives of γ-PGA can be used to create tissue-engineering scaffolds that promote cell adhesion and support osteogenic differentiation of human mesenchymal stem cells.[37] The ability to tune the mechanical properties of tissue-engineering scaffolds is an important design feature as cellular behavior has been found to be heavily influenced by the mechanical properties of the surrounding environment.[38] In our system we alter the concentration of the hybrid peptide−polymer, the grafting density of the β-sheet peptide, and the ratio of the covalently coupled versus uncoupled peptide to tailor the mechanical properties of the gel. We also evaluate the hydrogel's response to cyclic loading and their recovery following the application of high strain environments. We utilized circular dichroism (CD), Fourier transform infrared spectroscopy (FTIR), and thioflavin T (ThT) binding techniques to probe the secondary structure in the polymer−peptide hybrid hydrogels. Following β-sheet conjugation, 85% or more of the carboxylic groups are available for further modifications, such as the cell adhesion peptide Arg-Gly-Asp (RGD), bioactive epitopes, or signaling moieties.

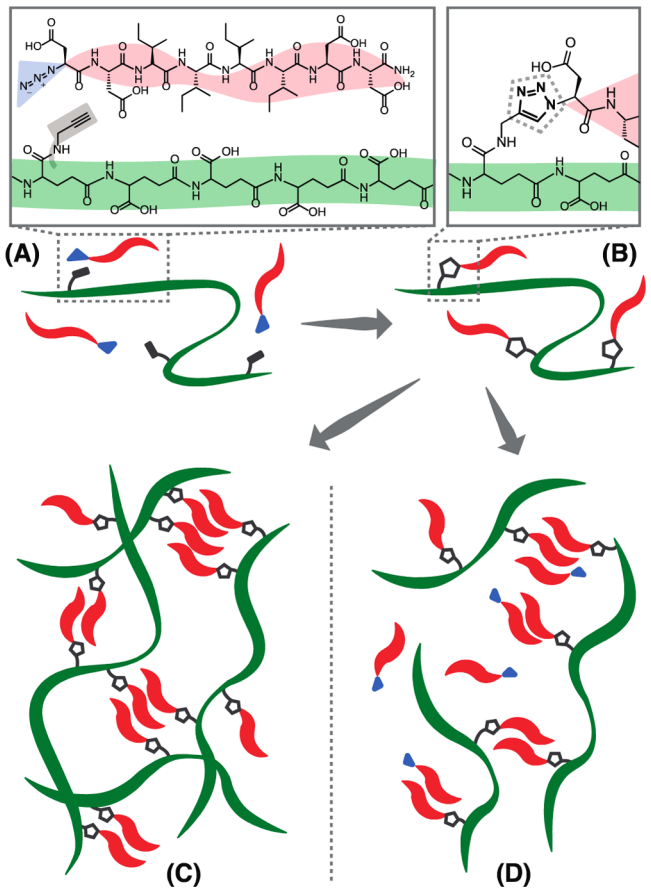

Figure 1. (A) Schematic of the azide-modified self-assembling β-sheet peptide (N_3-$D_2I_4D_2$) and alkyne-functionalized γ-PGA biopolymer. Synthesis and assembly of the hybrid hydrogel through mixing of azido-peptide and alkyne-polymer was followed by the copper-catalyzed click reaction (B) and assembly of β-sheets, inducing hydrogel formation. These hydrogels can be made to contain β-sheets that are covalently coupled to the polymer backbone (βC, shown in part C) and a controlled mixture of covalently coupled β-sheet peptides with uncoupled "free" β-sheet peptides (βF, shown in part D).

RESULTS AND DISCUSSION

Hybrid Hydrogel Formation. Hybrid hydrogels were synthesized from β-sheet forming peptides with an N-terminal azide (N_3-$D_2I_4D_2$) and γ-PGA, which had approximately 15% of the carboxylic acids modified with an alkyne (Figure 1A). The β-sheet peptide sequences were designed to contain a central region of four isoleucine residues, an amino acid with a high propensity to form β-sheets.[39,40] This central region is flanked by two aspartic acid residues on either side, which enhance the solubility of the hydrophobic isoleucines. These polymers were then mixed with azide-modified peptides, and copper-catalyzed click chemistry was used to click the peptides to the polymer and functionalize 5%, 10%, or 15% of the repeat units, referred to as γ-PGA-5%βC, γ-PGA-10%βC, and γ-PGA-15%βC, respectively (Figure 1B), and coupled using standard copper-catalyzed click chemistry (Figure 1C). After coupling these materials were dissolved in dimethyl sulfoxide (DMSO) at the desired concentration, pipetted into a dialysis tube, and dialyzed for over 24 h to remove the DMSO and any remaining copper, during which time the hydrogel formed in the tube. Under aqueous conditions, the peptide grafts were expected to self-assemble, providing physical cross-links of the hydrophilic polymer chain, resulting in the formation of a hydrogel. The hydrogel does not significantly swell during dialysis (Table S1), and inductively coupled plasma optical emission spectroscopy (ICP-OES) showed that the concentration of copper remaining in the hydrogels is below the detection limit (Figure S4). We also made hydrogels which had a mixture of covalently coupled and unbound peptides to see if adding in "free" peptide can be used to modify the mechanical properties of the hydrogel. In these hydrogels there was a constant 15% functionalization equivalent, but with either 5% or 10% of the peptide covalently coupled, with the remaining peptide free (Figure 1D). These are referred to as γ-PGA-5%βC+10%βF and γ-PGA-10%βC +5%βF. This series of materials allows us to study the effects of peptide functionalization, coupled versus uncoupled peptides, and concentration on the mechanical properties of self-assembled peptide−polymer hydrogels.

Analysis of Secondary Structure. Circular dichroism was performed to better understand the secondary structure of the hybrid hydrogels. In previous work on similar polymer-β-sheet hybrid networks, the CD showed a minimum around 218 nm, which is indicative of the β-sheet conformation.[31,41−43] In our

DOI: 10.1021/jacs.7b00528
J. Am. Chem. Soc. 2017, 139, 7250−7255

studies, γ-PGA had a CD spectra consisting of a minimum at 206 nm and reached a positive maximum at 195 nm (Figure 2A). Depending on its bacterial origin, γ-PGA predominantly formed from either D- or L-glutamic acid units, or a mixture of both. Previous studies have shown that γ-PGA can adopt ordered structures and generate a CD signal.[44,45] The CD spectra of *Bacillus subtilis* derived γ-PGA used in this study has a spectrum similar to that of the γ-PGA species that predominantly consist of D-glutamate stretches. Since γ-PGA itself generated a CD signal, this complicates the analysis of the spectra of the hydrogels, as both the polymer backbone and peptide components will contribute to the overall CD signature. Following β-sheet peptide conjugation, the CD had a minimum between around 220 and 230 nm for all samples, which is within the typical range for negative minima in β-sheet-forming systems (218−230 nm) and is thought to be representative of a β-sheet conformation of the attached peptide. This is interesting as even at the lowest β-sheet peptide concentrations (γ-PGA-5%βC) only 26% of the conjugate is peptide (by mass), while the remaining part is the γ-PGA polymer, yet the CD signal seems to be dominated by the self-assembling peptide. In this hybrid hydrogel, a larger fraction of β-sheet peptide leads to a red-shifting of the CD signal, which suggests that γ-PGA could be influencing the spectra by blue-shifting the CD signal more closely to that of the γ-PGA alone.

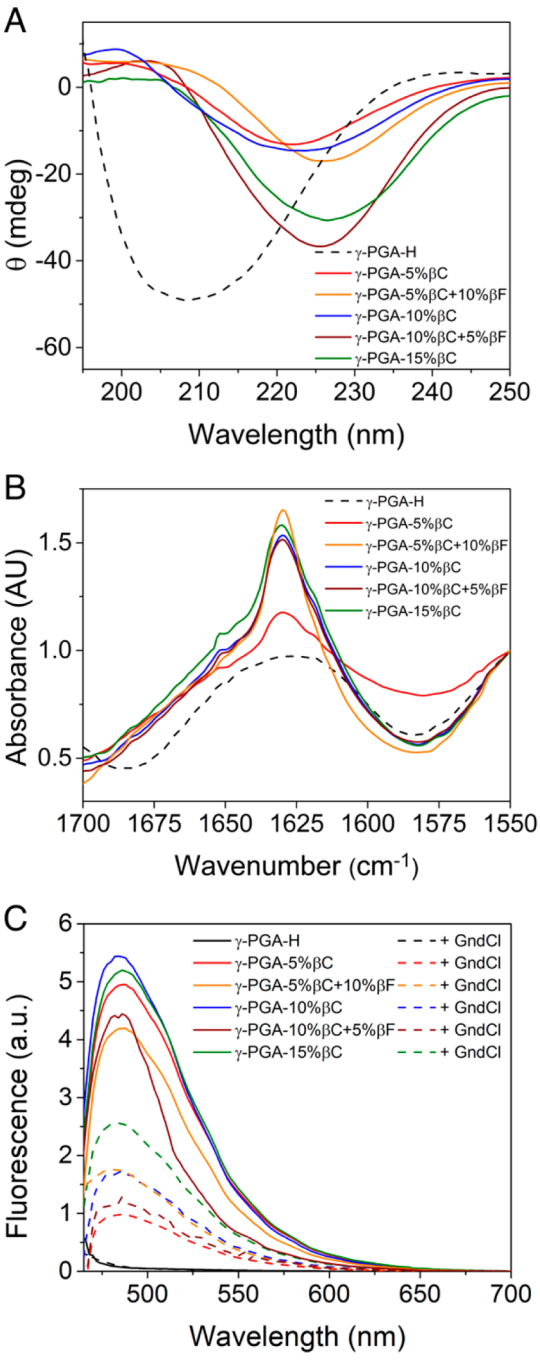

Figure 2. Spectroscopic studies of the hybrid hydrogels. (A) CD spectra showing minima for hybrid hydrogels between 220 and 230 nm, typically indicative of β-sheet formation. (B) FTIR spectra of the amide I region. (C) Thioflavin T assay, indicating the presence of β-sheets in the hydrogels that is greatly reduced in the presence of guanidinium chloride. All hydrogels were made 7.5% hybrid hydrogel by weight. FTIR studies in part C were performed on lyophilized hydrogels.

When investigating the secondary structure of γ-PGA grafted with β-sheet peptides, it should be noted that the γ-PGA and β-sheet peptides will not only contribute to the CD signal themselves, but they can modify the conformation of the polymer backbone and the peptide, making determination of the contributions of the individual parts difficult. Furthermore, β-sheet peptides generally adopt conformations that minimize their own free energy; however, in our systems some or all of the peptides are covalently tethered to a polymer which itself exerts forces on the β-sheet.

Fourier Transform Infrared Spectroscopy. FTIR was used to further verify the presence of the β-sheet secondary structure in the hybrid hydrogels. The amide I peak is sensitive to secondary structure, and its presence at 1630 cm^{-1} indicates a β-sheet conformation.[46,47] As seen in Figure 2B, a prominent peak at 1630 cm^{-1} is displayed in all the synthesized hybrid hydrogels and is not present in the γ-PGA spectra. FTIR performed on the γ-PGA-10%βC in both D_2O and in the dried state had similar spectra, indicating that our results are representative of the hydrated hydrogel (Figure S5).

Thioflavin T Binding Studies. ThT is a benzothiazole which increases in fluorescence when bound to β-sheet-rich structures.[48] This was also used to verify the presence of β-sheets and has the advantage of having low background from other polypeptide secondary structures, such as γ-PGA-alkyne, which can influence other spectroscopic techniques.[49,50] As seen in Figure 2C, exciting the hydrogels at 440 nm showed an enhancement in ThT fluorescence at 485 nm compared to γ-PGA, which did not have a peak. Interestingly, the mixtures of free and bound peptide have lower ThT signals than the hybrid hydrogels with only bound peptide, suggesting that having peptides tethered to polymers may change the β-sheet conformation in a way which effects ThT binding. To verify that β-sheet structures were responsible for the ThT signal, the hybrid hydrogels were incubated with 6 M guanidinium chloride (GndCl), a β-sheet denaturant. The resulting spectra show a significant loss of the 485 nm peak for all the hybrid hydrogels (Figure 2C).

Mechanical Characterization. The mechanical properties of the hydrogels were studied using oscillatory shear rheology. In this, the storage modulus (G') (elastic component) and loss modulus (G'') (viscous component) were observed as a function of both oscillation frequency and strain. For all the materials that formed self-supporting hydrogels, the storage modulus exceeded the loss modulus, indicating the formation

DOI: 10.1021/jacs.7b00528
J. Am. Chem. Soc. 2017, 139, 7250−7255

of a gel. From the frequency sweeps (Figure S6B) it is seen that the mechanical properties of the hybrid hydrogel are relatively independent of oscillation frequency. The mechanical properties of the hydrogels remained in the linear elastic region up to strains of around 10% with little change in the storage modulus, followed by a significant decrease in storage modulus for strains exceeding 20% (Figure S6A,D).

The mechanical properties of the hybrid hydrogels were found to be dependent on the concentration of the hydrogel, the β-sheet peptide graft density, and the ratio of coupled peptides to free peptides. The stiffness of the hydrogels could be varied by over an order of magnitude through changing concentration as seen in Figure 3A. Comparing the stiffness of

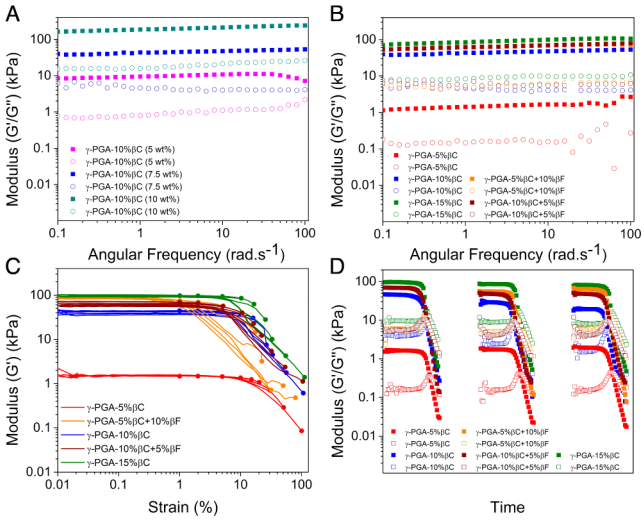

Figure 3. (A) Frequency sweep of the γ-PGA-10%βC hybrid hydrogel at different concentrations (5, 7.5, and 10 wt%). (B) Mechanical properties of the hybrid-hydrogels can be controlled using both grafting density and ratio of bound and unbound β-sheet peptide. (C) Cyclic sweeps of increasing strain from 0 to 0.01%, 1%, 2%, 5%, 10%, 15%, 20%, 30%, 50%, and 100%), with a point representing the last point of each strain sweep. (D) Three repeat strain sweeps from zero to 200% strain at an oscillation frequency of 6.283 rad s^{-1} with a 30 min recovery period in between each sweep for all of the hybrid hydrogels, showing that gels are able to recover their mechanical properties after failure. All samples are 7.5% hybrid hydrogel by weight unless otherwise noted.

γ-PGA-10%βC (5 wt%), γ-PGA-10%βC (7.5 wt%), and γ-PGA-10%βC (10 wt%), it is seen that the modulus of the hydrogels increases significantly with increased hydrogel concentration, from 10 kPa to over 200 kPa, while keeping other mechanical properties, such as failure strain, constant. These stiffness values are in the region of many soft tissues and compare well to those from previously published peptide−polymer hybrid hydrogel systems.[20−22,31−34]

One of the benefits of using peptide−polymer hybrid hydrogel systems is that the high-molecular-weight polymer backbone should help to reinforce the self-assembled β-sheets in the gel, helping the gel maintain its mechanical properties when exposed to significant strain. The failure strain of hydrogel systems can be defined as the point where the loss modulus surpasses the storage modulus and the gel becomes a viscous liquid.

In biological environments, materials will need to be able to withstand mechanical deformation from both exogenous strains placed on the entire biomaterial and the forces cells exert on their local matrix. To further characterize the ability of our gels to recover from moderate deformation, we placed them under a series of immediately increasing strains and monitored the effect on storage and loss moduli. Figure 3C shows the evolution of storage moduli of the hybrid hydrogels for these series of strain sweeps. Hybrid hydrogels typically do not lose any mechanical integrity until strains up to 20%. However, it is notable that the γ-PGA-10%βC+5%βF and especially 5%βC +10%βF start yielding at lower strains than those hydrogels that consist solely of covalently coupled peptides (Figure 3C). In these systems either one-third or two-thirds of the peptides are not covalently attached to the polymer backbone and should be less hindered to assemble into nanostructures. This suggests that the benefits of covalently bonding all peptides to the backbone outweigh any ability that free peptides have in helping to form nanostructural conformations that would not be available to a system with all covalently bound peptides. These covalently bonded hydrogels help the system to resist strain without losing mechanical properties. Interestingly, changing the ratio of covalently bound and free peptides in the system allows for tuning the yield strain in the hydrogels independently of storage modulus, which is not possible by changing either hydrogel or peptide concentration.

Figure 3C and Figure S6A,D show that the storage modulus of some hydrogels began to drop slightly for each individual sweep for larger strains, with the final values of G' typically falling to 80% of their initial value. This again highlights the ability for these hybrid hydrogels to maintain mechanical integrity. In this system, the plastic deformation at larger strains is gradual rather than catastrophic, and the ability to recover mechanical properties after large strains is rapid, as there are no waiting periods in between subsequent strains in this study.

One of the primary benefits of using non-covalent rather than covalent interactions is the ability of the bonds to reform after failure. Thus, after the application of high strains, the hybrid hydrogels would quickly recover their mechanical properties. To test this, we performed three individual strain sweeps to 200% with 30 min recovery periods in between the strains (Figure 3D). Some gels in this study had storage moduli that matched the initial moduli of the first strain sweep. There was also a large recovery in the failure strains, which ranged from 81% to 100% of the first strain sweep. The ability of these materials to self-heal indicates that the non-covalent β-sheets are able to rapidly reform in situ after breaking during large strains. The fact that they retain a larger percentage of their initial mechanical properties after a 30 min recovery period versus immediate strain to failure (around 70%) underscores the dynamic nature of the hybrid hydrogels, as the β-sheets are able to adopt more energetically favorable and mechanically robust conformations over time. The self-healing characteristic and the resistance to cyclic stain render these hybrid hydrogels ideal for biomedical applications which require recovery after significant deformation, such as injectable therapies, or include cell types which exert significant strain on their environment. We performed rheological testing on the γ-PGA-10%βC (7.5 wt%) hydrogel with physiological salt concentration and found that it retained the majority of its mechanical properties, with a storage modulus of 35 kPa, compared to 45 kPa for hydrogels in ultrapure water (Figure S7). To ensure that our hydrogels supported cell attachment and viability, we cultured human dermal fibroblasts on the γ-PGA-10%βC (7.5 wt%) hydrogel and found that the cells were able to adhere and were viable (Figure S8).

DOI: 10.1021/jacs.7b00528
J. Am. Chem. Soc. 2017, 139, 7250−7255

Scanning Electron Microscopy. The peptide–polymer hybrids form opaque hydrogels that can be manipulated with tweezers (Figure S9A). To better understand the nanostructure of the hybrid hydrogels, the materials were dehydrated via critical point drying and imaged using scanning electron microscopy (SEM). The SEM images showed that all the hybrid hydrogels have a highly porous structure formed from a connected network of fibers, as shown in Figures 4 and S9.

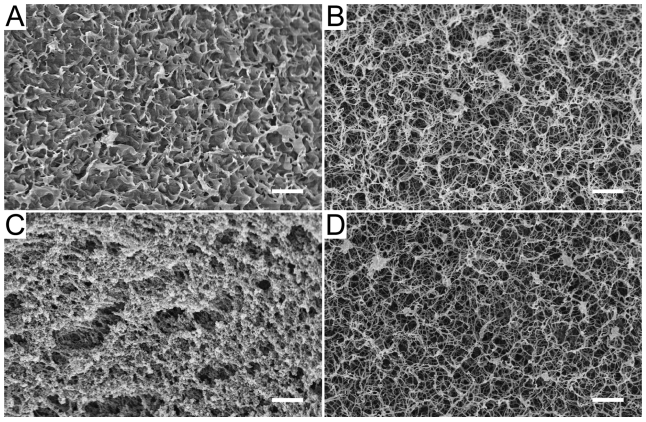

Figure 4. SEM images of (A) γ-PGA-5%βC, (B) γ-PGA-10%βC, (C) γ-PGA-15%βC, and (D) γ-PGA-10%βC + 5%βF. All hydrogels are 7.5% hybrid hydrogel by weight, and the scale bar is 1 μm.

Hydrogels that had higher amounts of γ-PGA, such as the γ-PGA-5%βC (Figure 4A) appeared to have more sheet-like nanostructures, while more peptide and free peptide containing hydrogels had an increased amount of high-aspect ratio fibrillar nanostructures.

CONCLUSIONS

In the work described in this paper we synthesized peptide–polymer hybrid hydrogels by grafting β-sheet peptides onto a poly(γ-glutamic acid) polymer backbone. We were able to tailor the stiffness of the hydrogels by changing the β-sheet peptide graft density, changing the bulk hydrogel concentration, and also changing the ratio of covalently coupled and free peptide. We were also able to create hydrogels with similar storage moduli but different abilities to maintain mechanical properties in response to strain. These β-sheet peptides act as strong physical cross-links, allowing the hydrogel to maintain mechanical properties over a series of increasing strains up to ∼20%. After being strained to failure, the hydrogel was able to heal through reassembly of β-sheet domains, which can reform due to their non-covalent nature. We used a variety of spectroscopic techniques to probe the secondary structure of the hybrid hydrogels, which indicated the formation of β-sheets. With gelation occurring at β-sheet peptide graft densities between 5% and 15% of the carboxylic acids on the poly(γ-glutamic acid) backbone, the hydrogels could be modified further with peptides and bioactive epitopes, such as the cell adhesion sequence Arg-Gly-Asp (RGD). Having the ability to incorporate additional functionality coupled with tailorable mechanical properties, this self-healing hybrid hydrogel serves as a promising platform for future tissue-engineering scaffolds and biomedical applications.

ASSOCIATED CONTENT

Supporting Information

The Supporting Information is available free of charge on the ACS Publications website at DOI: 10.1021/jacs.7b00528.

LC-MS of the N_3-$D_2I_4D_2$ peptide (Figure S1), NMR peak assignments (Figure S2) and spectra (Figure S3) for all materials, ICP-MS on hydrogel for copper (Figure S4), additional spectroscopic studies (Figure S5), additional rheological studies (Figures S6 and S7), fluorescent microscopy of cells on hydrogels (Figure S8), and SEM images (Figure S9), along with a summary of the hydrogel swelling study (Table S1) and experimental details (PDF)

Raw data is available on request from m.stevens@imperial.ac.uk.

AUTHOR INFORMATION

Corresponding Author

*m.stevens@imperial.ac.uk

ORCID

David E. Clarke: 0000-0003-0754-8928
E. Thomas Pashuck: 0000-0003-2881-4965
Sergio Bertazzo: 0000-0003-4889-8190
Molly M. Stevens: 0000-0002-7335-266X

Author Contributions

‖D.E.C. and E.T.P. contributed equally.

Notes

The authors declare no competing financial interest.

⊥J.V.M.W.: Deceased.

ACKNOWLEDGMENTS

D.E.C. was funded through a BBSRC case studentship BB/F018312/1, E.T.P. was funded through a Marie Curie International Fellowship "Peptide Osteogel" under grant agreement no. 275433, S.B. was supported by the Junior Research Fellowship scheme at Imperial College London, and M.M.S. would like to thank ERC starting investigator grant "Naturale" under grant number 206807 and the Rosetrees Trust for funding. We would like to acknowledge Cristina Gentilini for chemistry assistance and useful discussions, Charalambos Kallepitis for assistance with the FTIR, Guanglu Wu for assistance with the artwork, and Alessandra Pinna for assistance with the ICP-OES. This article is dedicated to the memory of Jonathan Weaver.

REFERENCES

(1) Place, E. S.; Evans, N. D.; Stevens, M. M. *Nat. Mater.* **2009**, *8*, 457–470.
(2) Li, J.; Suo, Z.; Vlassak, J. J. *J. Mater. Chem. B* **2014**, *2* (39), 6708.
(3) Fan, C.; Liao, L.; Zhang, C.; Liu, L. *J. Mater. Chem. B* **2013**, *1* (34), 4251.
(4) Haines-Butterick, L.; Rajagopal, K.; Branco, M.; Salick, D.; Rughani, R.; Pilarz, M.; Lamm, M. S.; Pochan, D. J.; Schneider, J. P. *Proc. Natl. Acad. Sci. U. S. A.* **2007**, *104* (19), 7791.
(5) Storrie, H.; Guler, M. O.; Abu-Amara, S. N.; Volberg, T.; Rao, M.; Geiger, B.; Stupp, S. I. *Biomaterials* **2007**, *28*, 4608–4618.
(6) Guler, M. O.; Hsu, L.; Soukasene, S.; Harrington, D. A.; Hulvat, J. F.; Stupp, S. I. *Biomacromolecules* **2006**, *7*, 1855–1863.
(7) Niece, K. L.; Hartgerink, J. D.; Donners, J. J. J. M.; Stupp, S. I. *J. Am. Chem. Soc.* **2003**, *125*, 7146–7147.
(8) Jung, J. P.; Moyano, J. V.; Collier, J. H. *Integr. Biol.* **2011**, *3*, 185–196.

DOI: 10.1021/jacs.7b00528
J. Am. Chem. Soc. 2017, 139, 7250–7255

(9) Fu, J.; Wang, Y.-K.; Yang, M. T.; Desai, R. A.; Yu, X.; Liu, Z.; Chen, C. S. *Nat. Methods* **2010**, *7*, 733−736.
(10) Hern, D. L.; Hubbell, J. A. *J. Biomed. Mater. Res.* **1998**, *39*, 266−276.
(11) Hersel, U.; Dahmen, C.; Kessler, H. *Biomaterials* **2003**, *24*, 4385−4415.
(12) Yang, F.; Williams, C. G.; Wang, D.; Lee, H.; Manson, P. N.; Elisseeff, J. *Biomaterials* **2005**, *26*, 5991−5998.
(13) Seliktar, D.; Zisch, A. H.; Lutolf, M. P.; Wrana, J. L.; Hubbell, J. A. *J. Biomed. Mater. Res.* **2004**, *68A*, 704−716.
(14) Cordier, P.; Tournilhac, F.; Soulié-Ziakovic, C.; Leibler, L. *Nature* **2008**, *451* (7181), 977−980.
(15) Kakuta, T.; Takashima, Y.; Harada, A. *Macromolecules* **2013**, *46* (11), 4575−4579.
(16) Wang, Q.; Mynar, J. L.; Yoshida, M.; Lee, E.; Lee, M.; Okuro, K.; Kinbara, K.; Aida, T. *Nature* **2010**, *463* (7279), 339−343.
(17) Burnworth, M.; Tang, L.; Kumpfer, J. R.; Duncan, A. J.; Beyer, F. L.; Fiore, G. L.; Rowan, S. J.; Weder, C. *Nature* **2011**, *472* (7343), 334−337.
(18) Burattini, S.; Greenland, B. W.; Merino, D. H.; Weng, W.; Seppala, J.; Colquhoun, H. M.; Hayes, W.; Mackay, M. E.; Hamley, I. W.; Rowan, S. J. *J. Am. Chem. Soc.* **2010**, *132* (34), 12051−12058.
(19) Rowland, M. J.; Atgie, M.; Hoogland, D.; Scherman, O. A. *Biomacromolecules* **2015**, *16* (8), 2436−2443.
(20) Kopeček, J.; Wang, C.; Stewart, R. J. *Nature* **1999**, *397* (6718), 417−420.
(21) Yang, J.; Xu, C.; Wang, C.; Kopeček, J. *Biomacromolecules* **2006**, *7* (4), 1187−1195.
(22) Dånmark, S.; Aronsson, C.; Aili, D. *Biomacromolecules* **2016**, *17* (6), 2260−2267.
(23) Elder, A. N.; Dangelo, N. M.; Kim, S. C.; Washburn, N. R. *Biomacromolecules* **2011**, *12* (7), 2610.
(24) Koga, T.; Taguchi, K.; Kobuke, Y.; Kinoshita, T.; Higuchi, M. *Chem. - Eur. J.* **2003**, *9* (5), 1146−1156.
(25) Higuchi, M.; Inoue, T.; Miyoshi, H.; Kawaguchi, M. *Langmuir* **2005**, *21* (24), 11462−11467.
(26) Burkoth, T. S.; Benzinger, T. L. S.; Urban, V.; Lynn, D. G.; Meredith, S. C.; Thiyagarajan, P. *J. Am. Chem. Soc.* **1999**, *121* (32), 7429−7430.
(27) Rösler, A.; Klok, H. A.; Hamley, I. W.; Castelletto, V.; Mykhaylyk, O. O. *Biomacromolecules* **2003**, *4*, 859−863.
(28) Hamley, I. W.; Ansari, I. A.; Castelletto, V.; Nuhn, H.; Rösler, A.; Klok, H. A. *Biomacromolecules* **2005**, *6* (3), 1310−1315.
(29) Hentschel, J.; Börner, H. G. *J. Am. Chem. Soc.* **2006**, *128*, 14142−14149.
(30) Börner, H. G.; Smarsly, B. M.; Hentschel, J.; Rank, A.; Schubert, R.; Geng, Y.; Discher, D. E.; Hellweg, T.; Brandt, A. *Macromolecules* **2008**, *41* (4), 1430−1437.
(31) Radu-Wu, L. C.; Yang, J.; Wu, K.; Kopeček, J. *Biomacromolecules* **2009**, *10*, 2319−2327.
(32) Wu, L. C.; Yang, J.; Kopeček, J. *Biomaterials* **2011**, *32*, 5341−5353.
(33) Maslovskis, A.; Guilbaud, J.-B.; Grillo, I.; Hodson, N.; Miller, A. F.; Saiani, A. *Langmuir* **2014**, *30* (34), 10471−10480.
(34) Ponnumallayan, P.; Fee, C. J. *Langmuir* **2014**, *30* (47), 14250−14256.
(35) Shih, I.-L.; Van, Y.-T. *Bioresour. Technol.* **2001**, *79* (3), 207−225.
(36) Akagi, T.; Wang, X.; Uto, T.; Baba, M.; Akashi, M. *Biomaterials* **2007**, *28*, 3427−3436.
(37) Gentilini, C.; Dong, Y.; May, J. R.; Goldoni, S.; Clarke, D. E.; Lee, B.-H.; Pashuck, E. T.; Stevens, M. M. *Adv. Healthcare Mater.* **2012**, *1*, 308−315.
(38) Discher, D. E.; Janmey, P.; Wang, Y. *Science* **2005**, *310*, 1139−1143.
(39) Chou, P. Y.; Fasman, G. D. *Biochemistry* **1974**, *13* (2), 222−245.
(40) Levitt, M. *Biochemistry* **1978**, *17* (20), 4277−4285.
(41) Radu, L. C.; Yang, J.; Kopeček, J. *Macromol. Biosci.* **2009**, *9*, 36−44.
(42) Castelletto, V.; Newby, G. E.; Zhu, Z.; Hamley, I. W.; Noirez, L. *Langmuir* **2010**, *26* (12), 9986−9996.
(43) Grieshaber, S. E.; Nie, T.; Yan, C.; Zhong, S.; Teller, S. S.; Clifton, R. J.; Pochan, D. J.; Kiick, K. L.; Jia, X. *Macromol. Chem. Phys.* **2011**, *212* (3), 229−239.
(44) Marlborough, D. I. *Biopolymers* **1973**, *12* (5), 1083−1088.
(45) Balasubramanian, D.; Kalita, C. C.; Kovacs, J. *Biopolymers* **1973**, *12* (5), 1089−1098.
(46) Byler, D. M.; Susi, H. *Biopolymers* **1986**, *25* (3), 469−487.
(47) Kubelka, J.; Keiderling, T. A. *J. Am. Chem. Soc.* **2001**, *123* (48), 12048−12058.
(48) Krebs, M.; Bromley, E.; Donald, A. M. *J. Struct. Biol.* **2005**, *149*, 30−37.
(49) Foderà, V.; Groenning, M.; Vetri, V.; Librizzi, F.; Spagnolo, S.; Cornett, C.; Olsen, L.; van de Weert, M.; Leone, M. *J. Phys. Chem. B* **2008**, *112* (47), 15174−15181.
(50) Biancalana, M.; Makabe, K.; Koide, A.; Koide, S. *J. Mol. Biol.* **2009**, *385* (4), 1052−1063.

DOI: 10.1021/jacs.7b00528
J. Am. Chem. Soc. 2017, 139, 7250−7255